ANALOG DEVICES

AN-1067
APPLICATION NOTE

One Technology Way • P.O. Box 9106 • Norwood, MA 02062-9106, U.S.A. • Tel: 781.329.4700 • Fax: 781.461.3113 • www.analog.com

The Power Spectral Density of Phase Noise and Jitter: Theory, Data Analysis, and Experimental Results

by Gil Engel

INTRODUCTION

Jitter on analog-to-digital and digital-to-analog converter sampling clocks presents a limit to the maximum signal-to-noise ratio that can be achieved (see *Integrated Analog-to-Digital and Digital-to-Analog Converters* by van de Plassche in the References section). In this application note, phase noise and jitter are defined. The power spectral density of phase noise and jitter is developed, time domain and frequency domain measurement techniques are described, limitations of laboratory equipment are explained, and correction factors to these techniques are provided. The theory presented is supported with experimental results applied to a real world problem.

GENERAL DESCRIPTION

There are numerous techniques for generating clocks used in electronic equipment. Circuits include R-C feedback circuits, timers, oscillators, and crystals and crystal oscillators. Depending on circuit requirements, less expensive sources with higher phase noise (jitter) may be acceptable. However, recent devices demand better clock performance and, consequently, more costly clock sources. Similar demands are placed on the spectral purity of signals sampled by converters, especially frequency synthesizers used as sources in the testing of current higher performance converters. In the following section, definitions of phase noise and jitter are presented. Then a mathematical derivation is developed relating phase noise and jitter to their frequency representation. The frequency domain representations, or power spectral densities, are shown to directly provide a measure of phase noise/jitter. The theory developed is associated with analog-to-digital and digital-to-analog converters. A spectrum analyzer and an oscilloscope are used to measure a variety of signals. Finally, theory is coupled with experimental results applied to an AD9235 analog-to-digital converter (ADC).

TABLE OF CONTENTS

REVISION HISTORY

4/10—Revision 0: Initial Version

DEFINITIONS

Phase noise and jitter have various interpretations. In the context of this application note, phase noise and jitter are defined as follows:

Consider the sinusoidal signal,

$$\sin(\omega t + A) \quad (1)$$

where:
$\omega = 2\pi f$.
f is the desired frequency.
A is a constant phase offset.

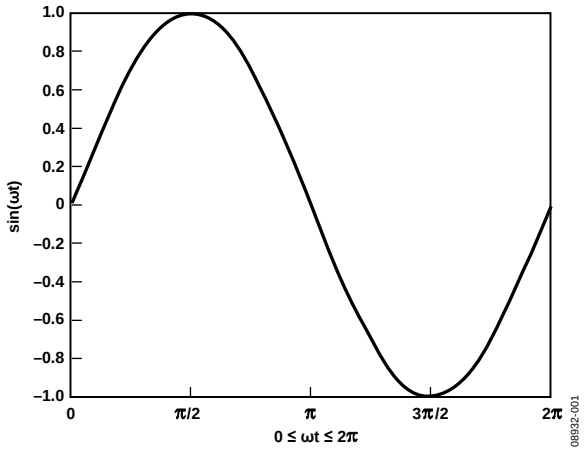

Figure 1. Normalized Sinusoidal Signal

PHASE NOISE

Phase noise is defined as an arbitrary function Φ(t) such that Equation 1 becomes

$$\sin(\omega t + A + \Phi(t)) \quad (2)$$

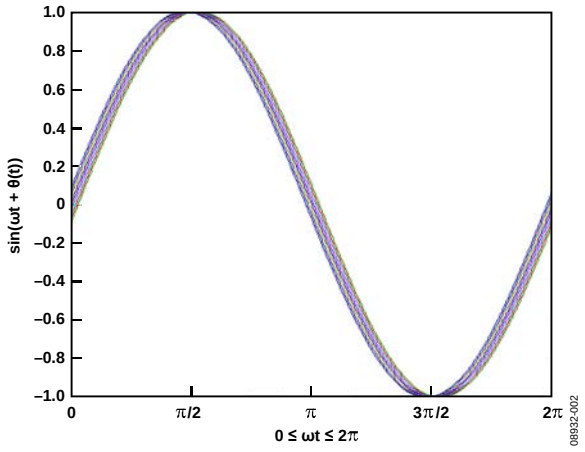

Figure 2. Sinusoidal Signal with Phase Noise

The function Φ(t) can be composed of frequency components not related to ωt, for example, thermal noise, shot noise, and 1/f noise (flicker noise). However, in most cases, it is modeled as Gaussian noise (see *Frequency Synthesizers Theory and Design Third Edition* by Manassewitsch in the References section).

Similarly, a sample clock can be considered a periodic square wave with rising and falling edges repeating at a fixed time interval, τ, such that

$$\tau = 1/f \quad (3)$$

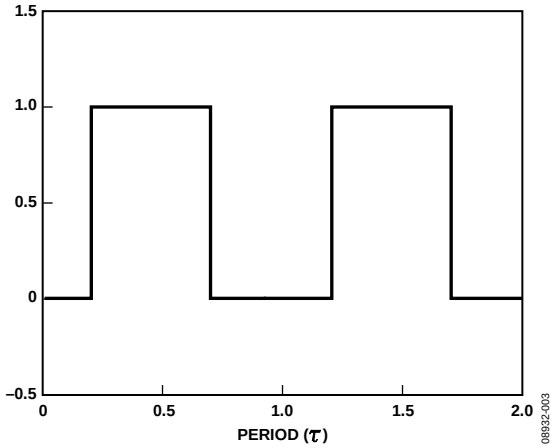

Figure 3. Sampling Clock

JITTER

Jitter can be defined as an additive time variation Δ(t) to the fixed interval τ, giving

$$\tau + \Delta(t) = 1/f + \Delta(t) \quad (4)$$

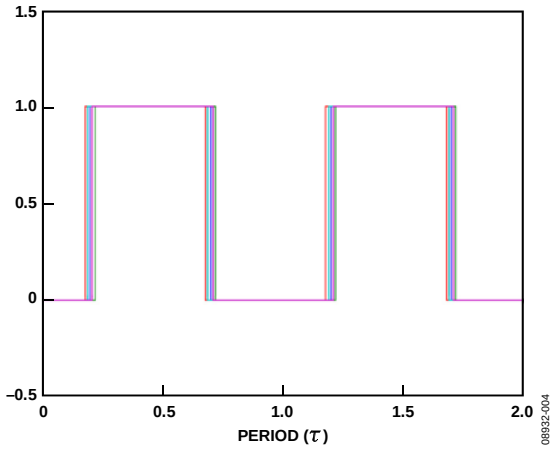

Figure 4. Sampling Clock with Jitter

Likewise, Δ(t), is typically characterized as Gaussian noise.

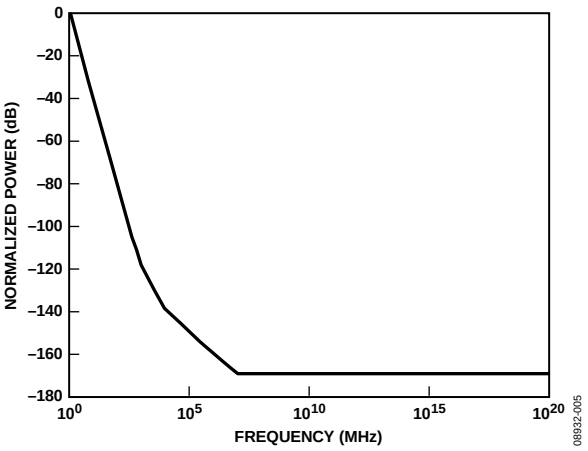

Figure 5. Single-Sideband Noise Spectrum of an Oscillator

Noise analysis is straightforward above 5 kHz until the active devices are limited at high frequency. Noise below 5 kHz exceeds the shot noise and thermal noise. This noise varies inversely with frequency and is identified as 1/f noise. Figure 5 shows a typical noise spectrum of an oscillator (see Manassewitsch in the References section).

POWER SPECTRAL DENSITY

Time domain signals have a direct relation to the frequency domain through the Fourier transform (see *Discrete-Time Signal Processing* by Oppenheim in the References section). The Fourier transform can be viewed as the magnitude and phase spectrum of a signal. A signal's power can also be viewed in the frequency domain. The power spectrum or power spectral density is given by

$$Syy(\omega) = Y(\omega) \times Y'(\omega) \quad (5)$$

where $Y(\omega)$ is the Fourier transform of $y(t)$.

As stated previously in the Definitions section, Φ(t) can be any arbitrary undesired signal. To simplify this analysis, Φ(t) is set to a single frequency. Consider the following:

$$\Phi(t) = \theta_d \sin\omega_m t \quad (6)$$

Such that Equation 2 becomes

$$y(t) = \sin(\omega_c t + \theta_d \sin\omega_m t) \quad (7)$$

The result is a phase-modulated signal, y(t), with maximum phase deviation in radians, θ_d, at a frequency, f_m, with $\omega_m = 2\pi f_m$, and no offset, A = 0.

The Jacobi-Anger expansion (see *Concise Encyclopedia of Mathematics* by Weisstein in the References section) states that

$$e^{iz\cos(\theta)} = \sum_{n=-\infty}^{\infty} i^n J_n(z) e^{in\theta} \quad (8)$$

or

$$e^{iz\sin(\theta)} = \sum_{n=-\infty}^{\infty} J_n(z) e^{in\theta} \quad (9)$$

can be manipulated with the help of Euler's identity to give

$$\cos(z\sin\theta) = J_0(z) + 2\times\sum_{n=1}^{\infty} J_{2n}(z)\cos(2n\theta) \quad (10)$$

and

$$\sin(z\sin\theta) = 2\times\sum_{n=1}^{\infty} J_{2n-1}(z)\cos[(2n-1)\theta] \quad (11)$$

where the $J_n(z)$ factors are Bessel functions of the first kind.

Using trigonometric identities, Equation 7, Equation 10, and Equation 11 can be manipulated to give

$$\begin{aligned} y(t) &= J_0(\theta_d)\sin(\omega_c t) \\ &+ J_1(\theta_d)[\sin(\omega_c + \omega_m)t - \sin(\omega_c - \omega_m)t] \\ &+ J_2(\theta_d)[\sin(\omega_c + 2\omega_m)t - \sin(\omega_c - 2\omega_m)t] \\ &+ J_3(\theta_d)[\sin(\omega_c + 3\omega_m)t - \sin(\omega_c - 3\omega_m)t] \\ &+ \ldots \end{aligned} \quad (12)$$

From Equation 12, it can be seen that y(t) has a first-order Bessel component at the carrier frequency, f_c, and Bessel-weighted signals at multiples of the modulation frequency, f_m, offset from the carrier.

The power spectral density, Syy(ω), of the function y(t) for f_c = 32,768 Hz and f_m = 1024 Hz with a phase deviation of 500 mrad (where mrad means milliradians) is shown in Figure 6.

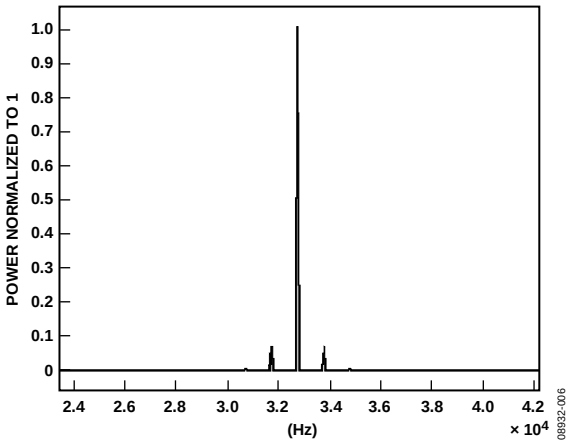

Figure 6. Power Spectral Density, Syy(ω)

Figure 6 is a plot of

$$Syy(\omega) = Y(\omega) \times Y'(\omega)$$

where $Y(\omega)$ is the Fourier Transform of $y(t)$.

Syy(ω) displays the magnitude of the power at the frequency, f. The power spectral density of the signal, y(t), modulated by a single frequency, f_m, only has components at f_c and f_m with Bessel-squared magnitudes.

The higher order Bessel coefficients attenuate very quickly. A log power scale provides better dynamic range, showing the higher order components in the same view as the large carrier component. The log of Syy(ω) is given by the following equation:

$$Lpy(\omega) = 10\log_{10}(Syy(\omega)) \quad (13)$$

and is shown in Figure 7.

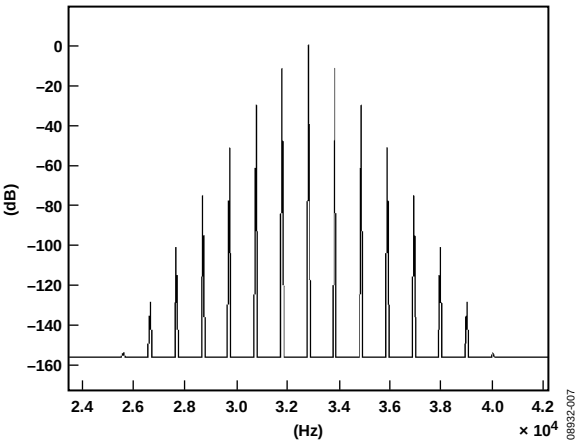

Figure 7. Log of Power Spectral Density, Syy(ω)

Additional terms are now clearly visible. As the phase deviation increases, the magnitude at the carrier frequency decreases and the magnitude of the modulation terms increases. 500 mrad of phase deviation reduces the carrier power by ~12%.

For small phase deviations, $\theta_d << 1$ rad, $J_0(\theta_d) \approx 1$, $J_1(\theta_d) \approx \theta_d/2$, and $J_2(\theta_d) \ldots J_n(\theta_d) \approx 0$ (see Manassewitsch in the References section).

As the phase deviation approaches zero, the carrier power approaches 100%. Furthermore, small phase deviations have a smaller percentage of the carrier frequency power distributed among the modulation terms. This, in turn, results in a sum of modulation terms that approximate the power of Φ(t) more accurately.

Bessel functions have the following property:

$$1 = J_0(\beta)^2 + 2\times\sum_{n=1}^{\infty} J_n(\beta)^2 \quad (14)$$

Taking advantage of the small phase deviation properties, the root mean square (rms) power of Φ(t) (for single-tone sinusoidal modulation) is approximately given by

$$P_{rm} \approx 2\times\sum_{n=1}^{\infty} J_n(\beta)^2 \quad (15)$$

or

$$P_{rms} \approx 1 - J_0(\beta)^2 \quad (16)$$

The phase deviation can also be expressed in terms of rms amplitude.

$$A_{rms} \approx \sqrt{P_{rms}} \quad (17)$$

EXAMPLE 1

For a phase deviation, θ_d, of 100 mrad,

$$P_{rms} \approx 1 - J_0(0.1)^2$$
$$P_{rms} \approx 1 - 0.9950094$$
$$P_{rms} \approx 1 - 0.0049906$$
$$A_{rms} \approx 0.0706444$$

Comparing this result with the power of a sinusoidal signal,

$$e(t) = A\sin(\omega t)$$
$$P_e = A^2/2$$

For A = 0.1, the rms power is $P_e = 0.005$ and $A_{rms} = A/\sqrt{2} = 0.0707107$, which confirms that, for small phase deviations, the modulating terms sum to provide a good approximation of the rms power.

This argument can be extended to more complex modulating signals. More complex modulation functions can be treated as a superposition of many frequency terms, each affecting the spectrum. The power spectral density has additional terms that sum to represent the rms power of the modulating signal. The rms power for an arbitrary function, Φ(t), with small amplitude, ($\theta_d << 1$ rad), is given by

$$P_{rms} = \int Syy(\omega)d\omega - Syy(\omega = \omega_c) \quad (18)$$

Equation 18 states that the rms power of a phase modulating signal is equal to the sum of all the components minus the power at the fundamental (or carrier frequency).

For a sinusoidal signal, y(t), phase modulation produces a symmetric power spectral density, such that the rms power can also be given by

$$P_{rms} = 2\times\int_{\omega>\omega_c}^{\infty} Syy(\omega)d\omega \quad (19)$$

This is referred to as a single-sideband measurement technique and is usually taken per root Hz (see Manassewitsch in the References section).

The rms modulation can be expressed in several ways.

$$A_{rms} \approx \sqrt{P_{rms}} \quad \text{in radians (shown in Equation 19)}$$
$$A^0_{rms} \approx 360 \times \sqrt{P_{rms}}/2\pi \quad (20)$$

Equation 20 expresses the phase deviation in degrees.

To relate phase noise to time jitter, use the following equation:

$$A^t_{rms} \approx \tau \times \sqrt{P_{rms}}/2\pi \quad (21)$$

where $\tau = 1/f_c$ expresses the phase deviation in time.

EXAMPLE 2—PHASE NOISE

Consider a noisy sinusoidal signal sampled with an ideal clock

$$y(t) = \sin(\omega_c t + N(t))$$

where:
$\omega_c = 2\pi 26{,}2144$.
$N(t)$ is Gaussian noise with a standard deviation, σ = 10 mrad.

The constructed signal is sampled at 4 million samples per second for 15 ms, acquiring 65,000 samples. The log of the power spectral density is normalized to 0 dB and is shown in Figure 8.

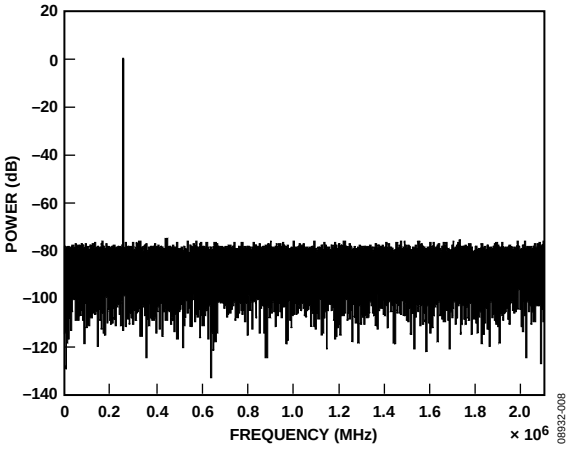

Figure 8. 260 kHz, 10 mrad Phase Noise

The fundamental is at around 260 kHz, and there is noise across the spectrum.

Using the discrete form of Equation 18,

$$P_{rms} = \sum_{n=0}^{N/2} Syy(n), \quad n \neq n_c \quad (22)$$

Sum the magnitude of the power at all frequencies from 0 to Nyquist, not including the power at the fundamental. The resulting noise power is

$$P_{rms} = 1.0017 \times 10^{-4}$$

The rms amplitude is $A_{rms} = 0.010008$ rad.

Note that the 0.008 mrad discrepancy is several orders of magnitude smaller than the exact rms noise amplitude of 10 mrad, giving a very good approximation.

The input signal at Time t_0 with a phase deviation of $\Phi(t_0) = 0$ has Amplitude A_0. A noisy input signal with phase deviation $\Phi(t_0) = \Delta_\Phi$mrad at Time t_0 has Amplitude A_Φ. By the same token, the input signal sampled at a time deviation, $t_1 = t_0 + \Delta_t$, has Amplitude A_τ.

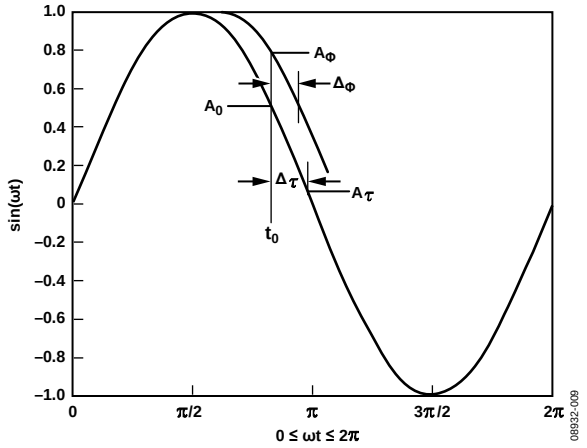

Figure 9. Effects of Timing and Phase Deviation on Sinusoidal Signal

Figure 9 shows that there exists a time deviation, Δ_t, and a phase deviation, Δ_Φ, that produce the same amplitude, A_Δ. For all intents and purposes, a phase deviation, Δ_Φ, with rms amplitude equal to the jitter, Δ_t, rms time deviation produces identical results.

EXAMPLE 3—JITTER

In Example 2, the power spectral density of a signal with phase noise, N(t), has a Gaussian distribution and standard deviation of σ = 10 mrad. Now consider a signal sampled with a jittery clock having Gaussian noise, η(t). Equation 21 can be used to determine the rms jitter to produce the same effect as 10 mrad of phase noise. The resulting output is

$$y(t) = \sin(\omega_c(t + \eta(t)))$$

where the carrier frequency is again 260 kHz and η(t) is Gaussian noise with a standard deviation of 6.0713 ns.

The constructed signal is sampled at 4M samples per second for 15 ms, acquiring 65k samples. The log of the power spectral density is normalized to 0 dB.

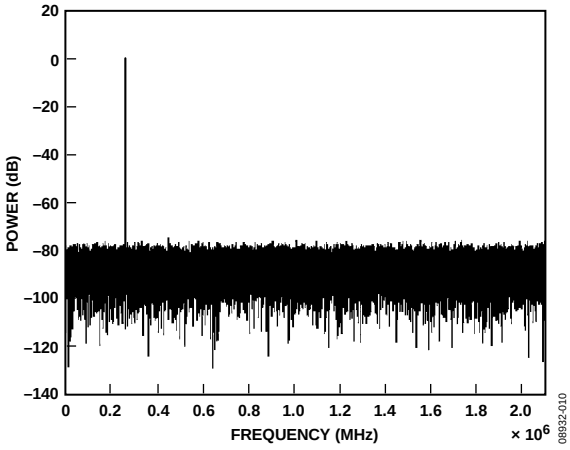

Figure 10. 65k FFT of a Phase Noise Modulated 260 kHz Tone Sampled at 4 MSPS

Using Equation 22, sum the magnitude of the power at all frequencies from 0 to Nyquist, not including the power at the fundamental. The resulting noise power is

$$P_{rms} = 1.0031 \times 10^{-4}$$

and the rms amplitude is

$$A_{rms} = 0.010016 \text{ rad}$$

Insert the results into Equation 21 to obtain

$$A^t_{rms} = 4.86455 \times 10^{-8}\text{s or } A^t_{rms} \approx 49 \text{ ns}$$

The results match those obtained in Example 2.

Broadband noise modulating the clock or input signal results in a power spectrum with distributed noise. Furthermore, noise modulating the input signal or clock produces symmetric noise about the carrier. The power spectral density can be used to determine the phase noise or jitter associated with specific frequency components or frequency ranges. Large symmetric terms may highlight specific frequencies that are modulating the signal and/or clock. The rms power associated with specific frequencies can be extracted directly from the power spectral density. For ranges of frequencies, the following equation can be used:

$$P_{rms} = \sum_{n=f_1}^{f_2} Syy(n) \quad (23)$$

Or for single sideband,

$$P_{rms} = 2 \times \int_{\omega_1}^{\omega_2} Syy(\omega) d\omega \quad (24)$$

APPLICATION TO CONVERTERS

Current high speed converters have sampling rates higher than 100 MSPS at resolutions greater than 12 bits. Signal-to-noise ratios (SNR) better than 70 dBc are routinely achieved with a spurious-free dynamic range (SFDR) better than 100 dBc. Digital-to-analog converter (DAC) performance is directly impacted by the sampling clock jitter. Tones produced by DACs sampled with a noisy clock can produce a signal with phase noise. ADCs are affected by noise on both the sampling clock and the input signal. The results derived in the Example 3—Jitter section can be applied to converters.

Associating the results to an ADC, consider the configuration shown in Figure 11.

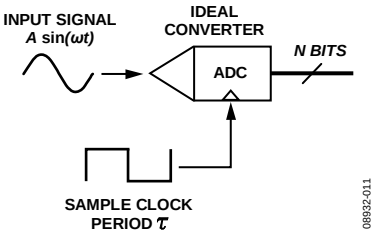

Figure 11. ADC Functional Block Diagram

The ADC samples the input signal, $A\sin(\omega t)$, at a time instant, t (having Period τ), producing a quantized output of N bits.

Assuming the noise on the input signal and the noise on the sampling clock are independent, the total noise is given by the root-sum square (RSS). If the magnitude of the noise is large enough, the maximum performance of the converter is affected.

The quantization noise is directly proportional to the number of bits. The maximum error a sample has within the ADC's range is the least significant bit resolution, Q_N, divided by 2 ($Q_N/2$) (see van de Plassche, Oppenheim, and *Delta-Sigma Data Converters Theory Design and Simulation* by Norsworthy, Schreier, and Temes in the References section). The error is defined by the signal being sampled. For randomly changing signals, the quantization error is uncorrelated and consequently lies anywhere within $\pm Q_N/2$. If the error is statistically independent of the signal being sampled, it can be shown that the maximum SNR that can be achieved is given by

$$SNR = 6.02N + 1.8 \quad (25)$$

For a 12-bit converter, the theoretical maximum SNR is ~74 dBc. A total quantization noise power of 74 dBc corresponds to

$$Pqn \approx 10^{-7.4}$$

$$Pqn \approx 39.8107 \times 10^{-9}$$

It is desirable to have a test setup that is 10 dB better than the converter being tested. To test a 12-bit converter, the desired test setup noise power is 84 dBc.

$$Pqn \approx 10^{-8.4}$$

$$Pqn \approx 3.98107 \times 10^{-9}$$

Using Equation 17, this noise power can be related to an rms phase deviation.

$$A_{rms} \approx 0.0631 \text{ mrad}$$

For a 10 MHz input signal, this corresponds to jitter of

$$A^t_{rms} \approx \tau \times \sqrt{P_{rms}}/2$$

$$A^t_{rms} \approx 100 \times 10^{-9} (\sqrt{3.98107 \times 10^{-9}})/2\pi$$

$$A^t_{rms} \approx 1.004 \times 10^{-12} \text{ sec}$$

Table 1 lists converter SNR limits due to quantization noise and comparable phase noise rms amplitude.

Table 1. Converter SNR Limits

Bit No.	Theoretical SNR Limit (dB)	Corresponding Phase Noise (mrad)	Test Setup	
			10 dB (mrad)	6 dB (mrad)
8	49.96	3.177	1.005	1.592
10	62	0.794	0.251	0.398
12	74.04	0.199	0.063	0.1
14	86.08	0.0497	0.016	0.025
16	98.12	0.0124	0.004	0.006

Table 1 also provides the phase noise rms amplitude for test setups at 10 dB and 6 dB better than the converter. In some cases, a test setup of 6 dB better than the converter is acceptable (especially when 10 dB is difficult to obtain).

Equivalent jitter amplitude is easily obtained using Equation 21.

Converter SNR performance is typically determined using the power spectral density. The sampling frequency and the number of data samples directly determine the frequency resolution. A 4k FFT for a converter sampling at 32 MHz accumulates enough data to resolve frequencies down to 8 kHz. Consequently, the power spectral density displays information in 8 kHz intervals. Each 8 kHz bin provides the sum of the power of the frequencies within that interval and frequencies aliased into that interval. The magnitude of a component that is 1 kHz from the carrier cannot be determined under these circumstances. The frequency resolution is improved by taking larger FFTs. Low frequency phase noise, such as 1/f noise, can be resolved to 32 Hz by taking a 1M FFT for a converter sampling at 32 MHz.

EXAMPLE 1

For a 12-bit ADC sampling at 32M samples per second with 20 ps of clock jitter, the input signal is at 4 MHz with a 2 kHz, 1 mrad phase noise component and 0.5 mrad of Gaussian phase noise. Acquiring 4k samples using this configuration produces the power spectral density shown in Figure 12.

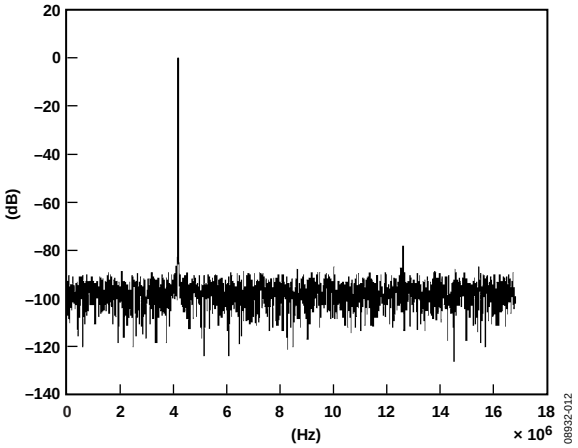

Figure 12. 4k FFT of a Modulated 4 MHz Tone Sampled at 32 MSPS

Using Equation 22, calculate a noise power of 6.628^{-7} W. However, the theoretical value should be 5.677^{-7} W, which is the RSS of the jitter and phase noise and quantization noise.

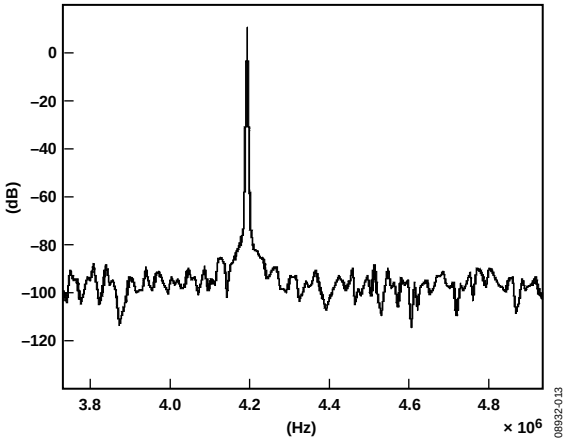

Figure 13. Close-Up View of 4 MHz Fundamental Showing Skirting Due to Low Bin Resolution

A close-up view (see Figure 13) shows skirting around the fundamental. The frequency resolution is 8 kHz, and the 2 kHz modulation terms have combined with the fundamental and the surrounding bins.

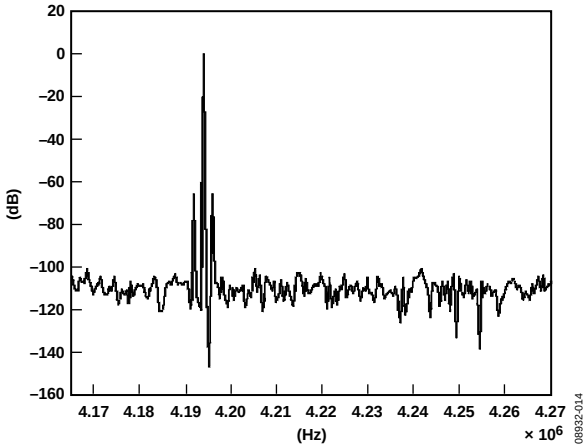

Figure 14. Higher Resolution FFT Showing Modulation Terms

Using a 65k FFT, the frequency can be resolved to 500 Hz. Two new symmetric terms are discovered, implying a phase modulation. Once these terms are added into the integrated noise power, calculate a noise power of 5.696^{-7} W.

TEST EQUIPMENT

Phase noise and jitter can be viewed as a time deviation using an oscilloscope or as a frequency spectrum using a spectrum analyzer.

OSCILLOSCOPES

Oscilloscopes fall into two categories: real-time and sampling (see *XYZs of Oscilloscopes* by Tektronix in the References section).

Real-time oscilloscopes capture a stream of samples on a single trigger event. The cycle-to-cycle deviation is extracted from the data at a fixed threshold. This method is limited by the time interval measurement accuracy of the oscilloscope and its internal jitter. The Tektronix TDS7404 specifies an accuracy of ±8.5 ps and a typical jitter noise floor of 1.5 ps rms. The Tektronix TDS694C has an accuracy of ±15 ps. Increased accuracy can be achieved with statistical methods by including the vertical resolution of the oscilloscope and large record lengths in the processing. Tektronix claims a 1.5 ps jitter measurement accuracy using the latter technique (see *Analyzing Clock Jitter Using Excel* and *Understanding and Performing Precise Jitter Analysis* by Tektronix in the References section).

Sampling oscilloscopes accumulate input signal data with each trigger. To obtain a time deviation, the input signal is repetitively sampled, acquiring a distribution of points at a horizontal cross-section. The horizontal and vertical scales are adjusted depending on the magnitude of the time deviation being measured. This method of time deviation measurement is mainly limited by the trigger jitter. Sampling oscilloscopes have a much better time interval accuracy and, more importantly, a sampling interval as low as 10 fs. The time interval accuracy of a Tektronix 11801C is 1 ps + 0.0004% × (position) and the trigger jitter is typically 1.1 ps rms. The TDS8000B Tektronix sampling oscilloscope specifies a trigger jitter of 800 fs (see *Automatic Measurement Algorithms and Methods for the 8000 Series Sampling Oscilloscopes* by Tektronix in the References section).

SPECTRUM ANALYZERS

Spectrum analyzers display a signal in terms of its frequency content. The spectrum displays a series of measurements within the resolution bandwidth (RBW) settings. Spectrum analyzers display the voltage and/or power of a signal in a linear or log display. Viewing the power of a signal is analogous to the power spectral density plots obtained through Fourier analysis.

Random noise in electronics has a Gaussian distribution. Therefore, samples within the RBW of the spectrum analyzer have a probability distribution; however, the samples are displayed as simple magnitudes. The spectrum analyzer actually measures with the in-phase (I) and quadrature (Q) components (see *Spectrum Analyzer Measurements and Noise* by Hewlett Packard in the References section). The I/Q components provide the magnitude and phase of the signal. Band-passed noise has a Gaussian distribution independently in both the I and Q components.

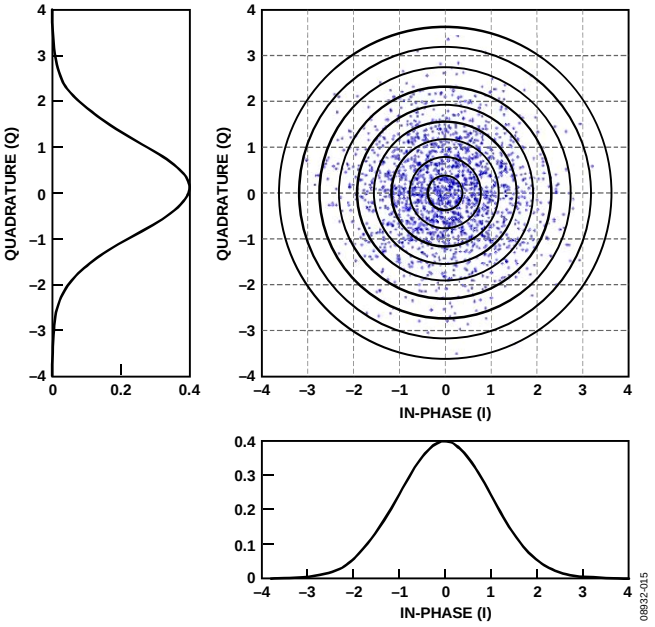

Figure 15. Spectrum Analyzer Envelope Detector Input Distribution

The magnitude is obtained with an envelope detector and is given by

$$v = \sqrt{v_I^2 + v_Q^2} \tag{26}$$

The noise magnitudes form concentric rings about the center of Figure 15. The count within each ring provides a distribution of the noise magnitude. The distribution function for the noise envelope is actually a Rayleigh distribution (see *Probability, Random Variables, and Stochastic Processes* by Papoulis in the References section).

$$D_{env}(v) = \frac{v}{\sigma^2} e^{-\frac{v^2}{2\sigma^2}} \tag{27}$$

Knowing the probability density function, the average of the voltage envelope can be determined using

$$\bar{v} = \int_0^\infty v D_{env}(v) dv = \sigma\sqrt{\frac{\pi}{2}} \tag{28}$$

The average power is given by

$$\bar{p} = \int_0^\infty \frac{v^2}{R} D_{env}(v) dv = \frac{2\sigma^2}{R} \tag{29}$$

Calculating the power by squaring the average envelope voltage then dividing by R does not provide the same results as Equation 29. The result is 1.05 dB smaller.

$$10\log\left(\frac{v^2/R}{\bar{p}}\right) = 10\log\left(\frac{\sigma^2 \pi R}{4\sigma^2 R}\right)$$

$$= 10\log\left(\frac{\pi}{4}\right)$$

$$= -1.05 \text{ dB}$$

Further considerations must be taken when using a spectrum analyzer in its logarithmic display mode. In the logarithmic display mode, the input signal passes through a log amplifier. This in turn results in a logged probability density function. Additionally, the spectrum analyzer displays an average of the log. Log processing results in a response to noise that is 2.51 dB lower.

PROOF

Proof of 2.51 dB underestimation of noise follows.

$$P_{\log} = 10\log(v^2) \text{ or } 20\log(v) \tag{30}$$

Take the derivative of both sides,

$$dp_{\log} = \frac{20}{\ln 10} \times \frac{1}{v} dv \tag{31}$$

$$v = 10^{\frac{P_{\log}}{20}} \tag{32}$$

and

$$dv = 10^{\frac{p_{\log}}{20}} \left(\frac{\ln 10}{20} \right) dp_{\log} \tag{33}$$

Use Liebniz's rule (see Weisstein in the References section)

$$f_y(y) = f_x(x)\frac{dx}{dy} \tag{34}$$

or per Papoulis (see the References section)

$$f_y(y) = \frac{f_x(x)}{dy/dx} \quad \text{at } x = T^{-1}\{y\} \tag{35}$$

To obtain

$$\begin{aligned} D_{\log}(p) &= \frac{D_{env}(v)}{dp_{\log}/dv} \quad \text{at } v = 10^{\frac{y}{20}} \\ &= \frac{10^{\frac{y}{20}} \times D_{env}(10^{\frac{y}{20}})}{20/\ln 10} \quad \text{at } v = 10^{\frac{y}{20}} \end{aligned} \tag{36}$$

The result is the probability distribution of log power of the input envelope.

The average log power is then given by

$$\overline{p_{\log}} = \int_{-\infty}^{\infty} p_{\log} D_{\log}(p_{\log}) dp_{\log} \tag{37}$$

From Liebniz's rule (and Papoulis)

$$f_y(y)dy = f_x(x)dx$$

Therefore,

$$\begin{aligned} \overline{p_{\log}} &= \int_0^{\infty} p_{\log} D_{env}(v) dv \\ &= \int_0^{\infty} 20\log(v) D_{env}(v) dv \\ &= \int_0^{\infty} 20\log(v) \frac{v}{\sigma^2} e^{-\frac{v^2}{2\sigma^2}} dv \end{aligned} \tag{38}$$

Let

$$\begin{aligned} 20\log(v) &= 10\log\left(\frac{2\sigma^2 v^2}{2\sigma^2} \right) \\ &= 10\log(2\sigma^2) + 10\log\left(\frac{v^2}{2\sigma^2} \right) \end{aligned} \tag{39}$$

To obtain

$$\begin{aligned} \overline{p_{\log}} &= 10\log(2\sigma^2) \int_0^{\infty} \frac{v}{\sigma^2} e^{-\frac{v^2}{2\sigma^2}} dv \\ &+ \int_0^{\infty} 10\log\left(\frac{v^2}{2\sigma^2} \right) \frac{v}{\sigma^2} e^{-\frac{v^2}{2\sigma^2}} dv \end{aligned} \tag{40}$$

The first integral goes to 1 because this is simply the integral of the Rayleigh probability density. Let

$$u = \frac{v}{\sigma^2} \tag{41}$$

in the second integral, giving

$$\overline{p_{\log}} = 10\log(2\sigma^2) + \frac{10}{\ln 10} \int_0^{\infty} \ln(u) e^{-u} du \tag{42}$$

The first term is the log of the average power; the second term is the negative of the Euler-Mascheroni constant (see Weisstein in the References section). The Euler-Mascheroni constant has been calculated to 7,000,000 digits and is denoted by Υ. Υ is approximately equal to 0.5772, making the last term equal to −2.5067.

Most modern spectrum analyzers feature noise measurements that apply the necessary correction factors.

In addition to known correction factors, which must be applied as necessary, spectrum analyzers must be configured correctly to provide accurate results. Smaller input signals are measured more accurately by lowering the reference level. However, lowering the reference level increases the gain of the input IF stage. Care must be taken so that the initial IF stage is not overloaded. Overloading the IF input sections may cause distortion products (see *Fundamentals of Spectrum Analysis* by Rauscher in the References section). Furthermore, finer frequency and amplitude resolution measurements are obtained by enhancing the resolution bandwidth (RBW) and video bandwidth (VBW), respectively. However, enhanced resolution comes at a cost of longer sweep times. Fortunately, software is available that takes the desired measurements and applies the appropriate correction factors.

LAB RESULTS

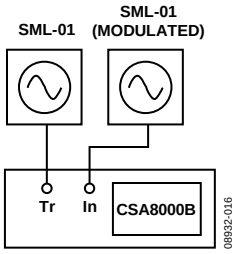

Figure 16. Oscilloscope Setup

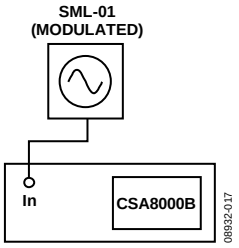

Figure 17. Spectrum Analyzer Setup

A modulated signal generated by a Rohde & Schwarz SML-01 was measured using a Tektronix CSA8000B and a Rohde & Schwarz FSIQ7. A second nonmodulated SML-01 set to the same frequency as the first SML-01 is used to trigger the CSA8000B. Phase noise due to large single-tone modulation, large Gaussian noise modulation, and small noise modulation was analyzed. In all cases, the source used is a Rohde & Schwarz SML-01.

An alternative oscilloscope setup uses a broadband resistive splitter to feed both the trigger and the sampling inputs. This method rejects low frequency noise, which may produce artificially low noise measurement results.

SIGNAL 1

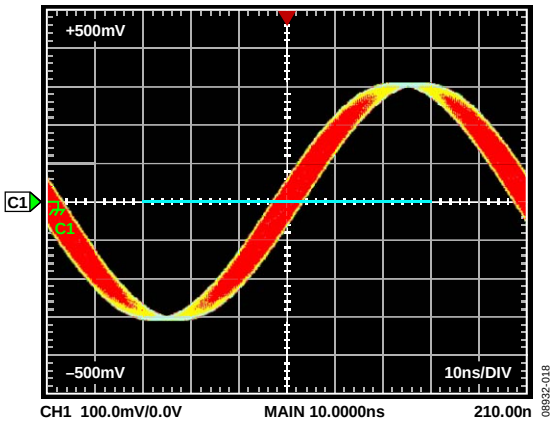

Figure 18. SML-01 at 10 MHz, Modulated 200 mrad at 101 kHz

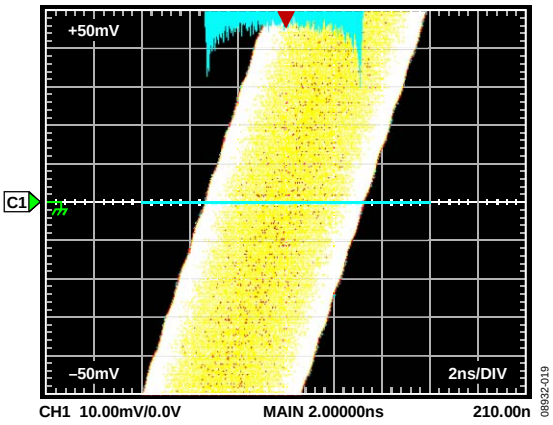

Figure 19. Close-Up View of Rising Edge

Taking a horizontal histogram at the rising edge cross-section displays a standard deviation in a time of 2.218 ns and a peak-to-peak deviation of 6.6 ns.

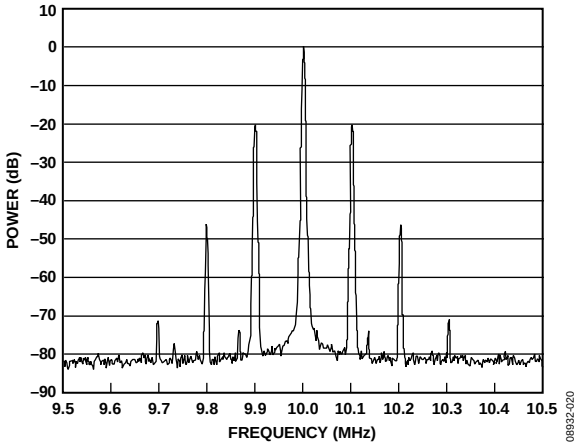

Figure 20. Single-Frequency Phase-Modulated Frequency

The spectrum analyzer clearly shows a spectrum due to single-frequency phase modulation. The first term to the right of the carrier has a Bessel factor of $J_1(\theta_d)$. Because $J_1(\theta_d) \approx \theta_d/2$, the modulation can be approximated at 200 mrad.

SIGNAL 2

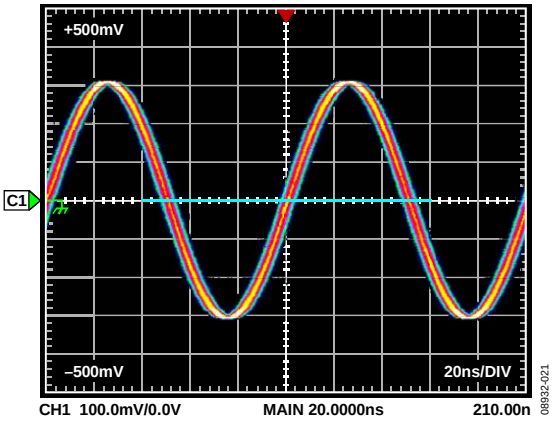

Figure 21. SML-01 at 10 MHz with 67 mrad RMS of Gaussian Noise Modulation

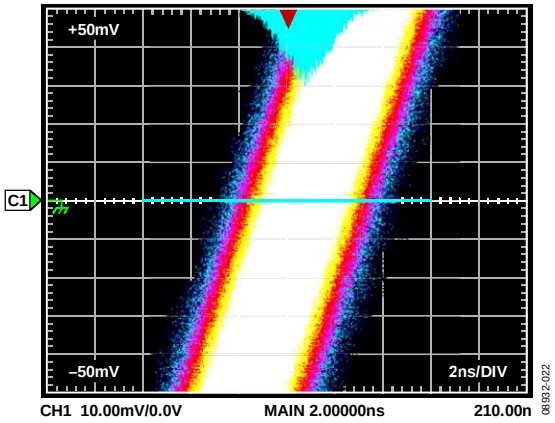

Figure 22. Close-Up View of Rising Edge

A horizontal histogram at the rising edge cross-section displays a standard deviation in a time of 1.005 ns and a peak-to-peak deviation of 7.92 ns. The oscilloscope trigger input accuracy decreases at lower slew rates.

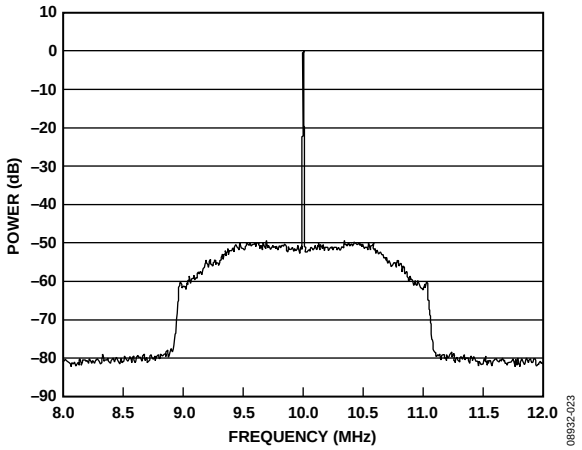

Figure 23. 10 MHz Signal with Noise Out to 1 MHz from Carrier

Figure 23 shows a spectrum due to broadband noise out to 1 MHz from the carrier. Using a single sideband phase noise measurement (see Equation 19), the calculated phase noise has an rms amplitude of 0.0676 radians, corresponding to about 1.075 ns of time jitter.

SIGNAL 3

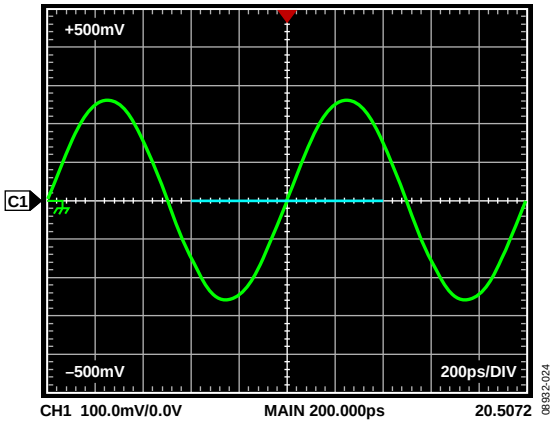

Figure 24. SML-01 Set to Produce a Clean 1 GHz

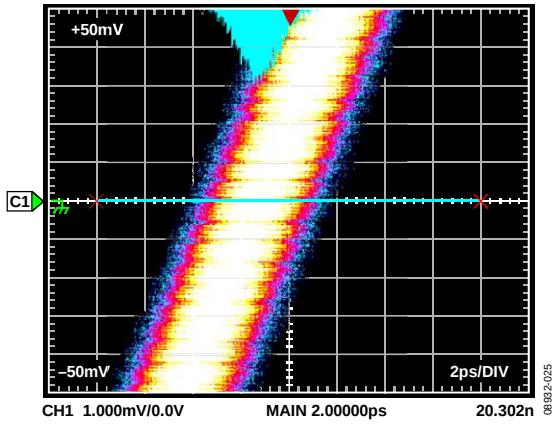

Figure 25. Close-Up View of Rising Edge

In this case, the deviation is so small that it is below the trigger jitter of the oscilloscope. The result shows a standard deviation of 837.3 fs and a peak-to-peak deviation of 5.56 ps.

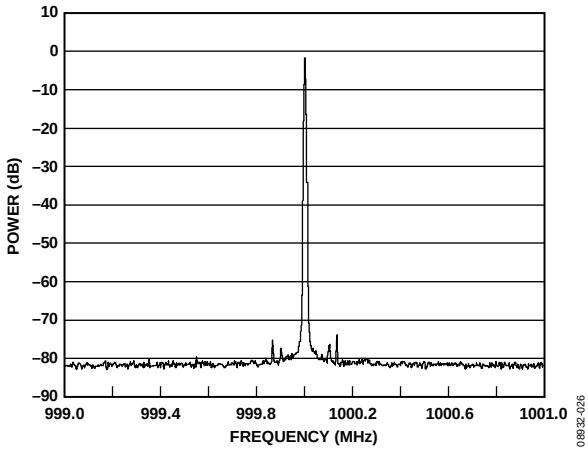

Figure 26. Full-Scale 1 GHz Signal with 1.6 mrad RMS of Phase Noise

The spectrum analyzer is centered at 1 GHz and set to a span of 2 MHz. The dynamic range can be enhanced by changing the frequency range so that the large carrier is outside the span.

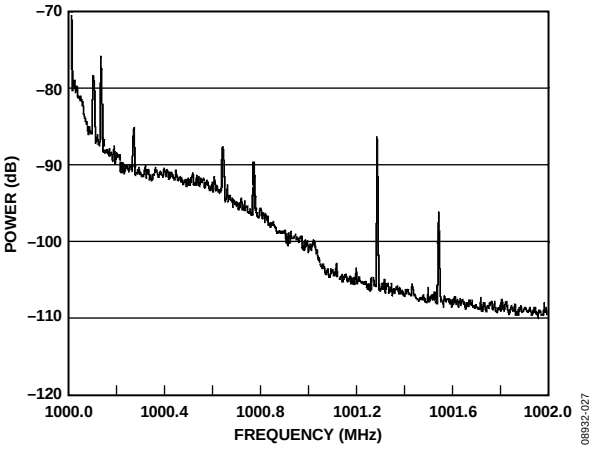

Figure 27. Single Sideband 1 GHz Signal with 1.6 mrad RMS Phase Noise

With the range now starting 5 kHz from the carrier, Figure 27 shows that there is broadband phase noise to 1 MHz from the carrier. A reference level that is too low causes the distortions appearing in Figure 27. To obtain accurate results, the measurements must be made in smaller intervals. Measurements within 10 kHz of the carrier must have a reference level that will not overload the input IF stage.

With a single sideband measurement (see Equation 19), the phase noise is measured at 1.6 mrad. This corresponds to 255 fs, far below the trigger jitter resolution of the oscilloscope.

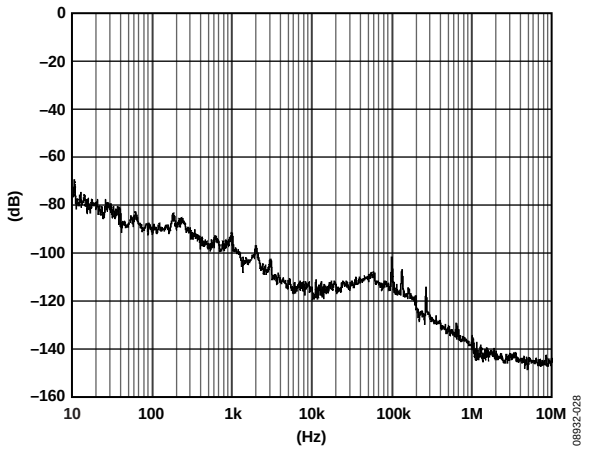

Figure 28. Single Sideband 1 GHz Signal with 1.6 mrad RMS Phase Noise and Nonoverloaded Input Stage

HIGH SPEED CONVERTER

Phase noise and jitter were introduced to an AD9235 application. The results obtained were verified using a spectrum analyzer and correlated to the developed theory. The AD9235 is a high speed analog-to-digital converter that features a 65M sample clock and SNR around 70 dBc. The experiment was executed on a CTS5340 tester. Rohde & Schwarz SMGUs generated both the input tone and clock. The input frequency was set to 2.4 MHz, and the clock input was set to 259.995 MHz divided down to produce a sampling rate, $f_s \approx 65$ MSPS. The sampling rate was decimated to produce an effective sampling rate, $f_{es} \approx f_s/15$.

The application normally generates an SNR around 70 dBc. A typical power spectral density, using a 4k FFT with the fundamental aliased into Bin 1827, is shown in Figure 29.

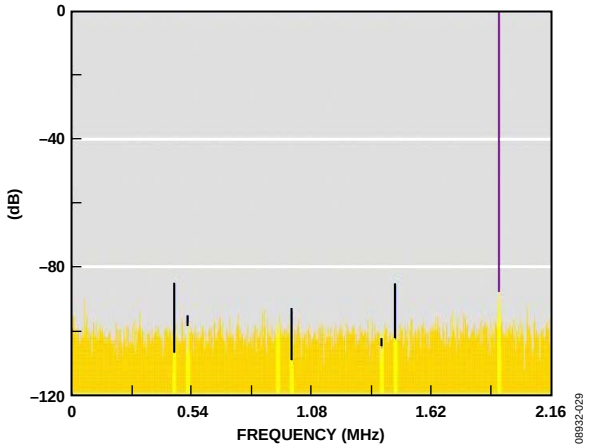

Figure 29. FFT of AD9235 ADC Application, Sample Rate Decimated to ~65 MSPS/15 and Input Frequency Set to 2.4 MHz

The signal $\Phi(t) = 0.01 \sin 2\pi 10{,}000t$ was modulated onto the fundamental. The resulting power spectral density is shown in Figure 30.

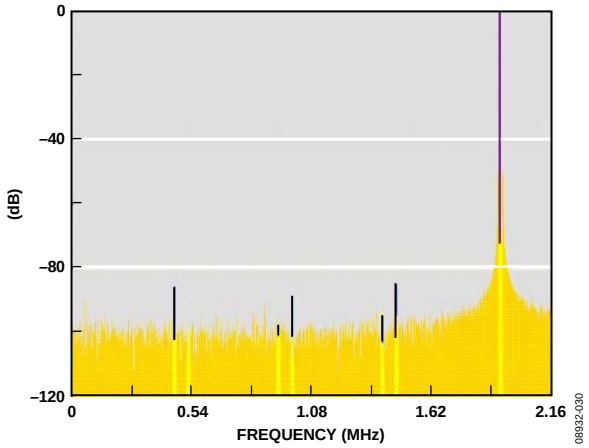

Figure 30. FFT of AD9235 ADC Application with a 10 kHz Tone Modulating the Fundamental

Figure 30 shows symmetric peaks about the fundamental, indicating a modulation. The bin width for the FFT is ~1057 Hz. Counting bins, the main peaks are found in the ninth and 10th bins from the fundamental, implying a modulation between 9.5 kHz and 10.5 kHz. The modulation term is spread out due to a sampling rate that is not a direct multiple of 10 kHz and a nonwindowed FFT. For small signal modulation (a safe assumption because the modulation peaks are more than 50 dBc), the first modulation Bessel term, $J_1(\theta_d)$, is approximately $\theta_d/2$. Sum the power for eight highest peaks around the modulation term to obtain

$$P_{J_1} \approx 2.0324 \times 10^{-5}$$

$$\theta_d/2 = \sqrt{P_{J_1}} \approx 0.0045$$

$$\theta_d = 0.009$$

Even though the modulation terms are spread throughout the spectrum, most of the modulation energy is centered around $f_c \pm f_m$. Summing eight terms results in an approximation within 10% of the actual value.

The power spectral density of a fundamental with added phase noise is shown in Figure 31.

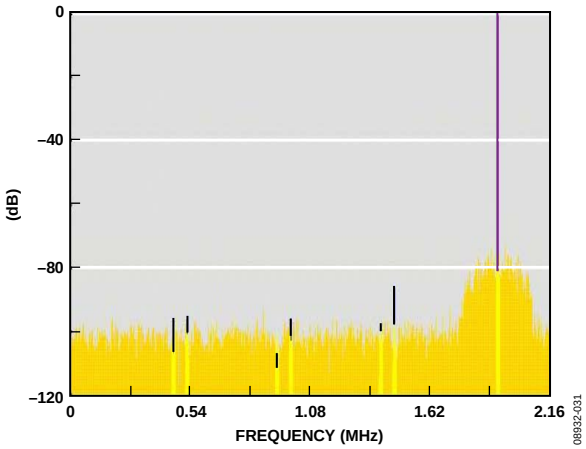

Figure 31. FFT of AD9235 ADC Application with Phase Noise Modulating the Fundamental

The CTS5340 tester sends a filtered signal to the application board. The equivalent noise bandwidth for the 2.4 MHz filter is approximately 300 kHz. The bandlimited noise is clearly seen around the fundamental, indicating phase modulated noise on the 2.4 MHz input tone. The phase noise results in an SNR of 58 dBc.

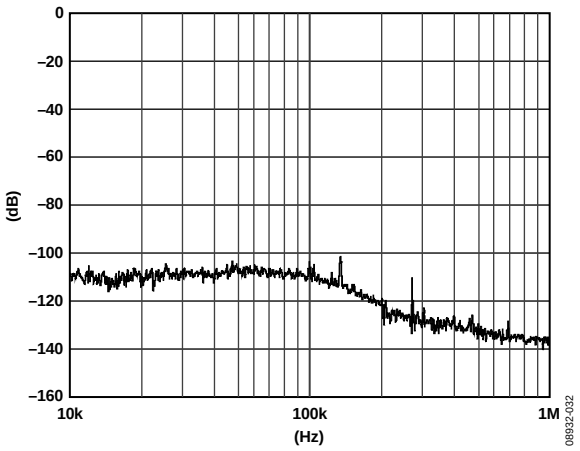

Figure 32. Single-Sideband Noise Spectrum of Fundamental with 1.5 mrad of Phase Noise

A single sideband measurement of the input signal shows 1.5 mrad of phase noise.

$$P_{rms} = A^2$$

$$P_{rms} = 2.25 \times 10^{-6} = -56.478 \text{ dB}$$

This matches the source phase noise with the application test results.

The results of jitter added to the sampling clock are shown in Figure 33.

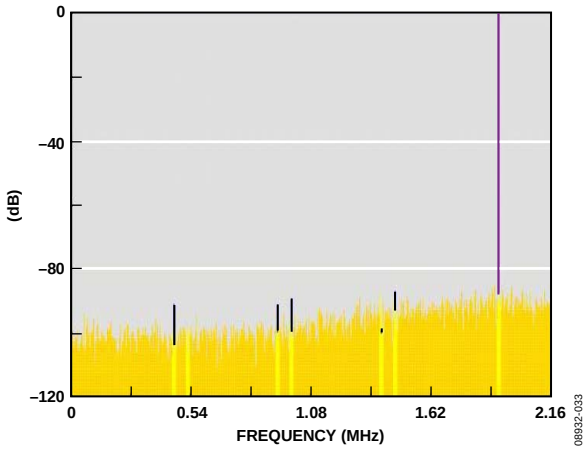

Figure 33. FFT of AD9235 ADC Application Sampled with Jitter Clock

In this case, the power spectral density noise floor has been slightly raised, resulting in an SNR of 64 dBc. The clock source is a Rohde & Schwarz SML-01 set to 259.995 MHz. A single sideband measurement of the SML-01 clock source is shown in Figure 34.

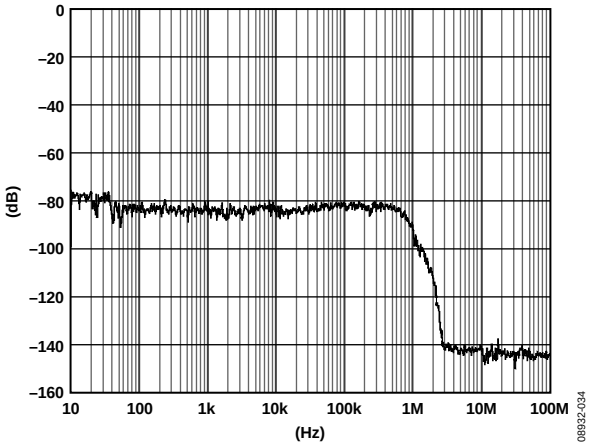

Figure 34. Phase Noise

The clock source has 66.9 mrad of phase noise.

$$A^t_{rms} = 0.0669/(2\pi 259.995 \times 10^6)$$
$$\approx 40.953 \text{ ps}$$

The phase noise on the sampling clock corresponds to about 41 ps of clock time jitter. The jitter can be related to radians of phase noise on the 2.4 MHz input signal.

$$A^t_{rms} = (40.953 \times 10^{-12}) \times (2\pi 2.4 \times 10^6)$$
$$\approx 0.618 \text{ mrad}$$

41 ps of clock jitter corresponds to 0.618 mrad of phase noise on the 2.4 MHz fundamental.

$$P_{rms} = A^2_{rms}$$

$$P_{rms} = 3.814 \times 10^{-7} = -64.187 \text{ dB}$$

The noise on the sampling clock matches the application test results.

CONCLUSION

The theory presented in this application note provides a direct relationship between phase noise and jitter and their frequency domain representation. Analysis of phase noise and jitter in the frequency domain highlights the content of the noise signals. Furthermore, measurements in the frequency domain provide enhanced resolution at higher frequencies.

REFERENCES

Hewlett Packard. 1998. Application Note 1303. *Spectrum Analyzer Measurements and Noise*.

Manassewitsch, Vadim. 1987. *Frequency Synthesizers Theory and Design Third Edition*. Wiley-Interscience.

Norsworthy, Steven, Richard Schreier and Gabor Temes. 1997. *Delta-Sigma Data Converters Theory Design and Simulation*. IEEE Press.

Oppenheim, Alan and Ronald W. Schafer. 1989. *Discrete-Time Signal Processing*. Prentice Hall.

Papoulis, Athanasios. 1984. *Probability, Random Variables, and Stochastic Processes*. McGraw-Hill.

Rauscher, Christoph. 2001. *Fundamentals of Spectrum Analysis*. Germany: Rohde & Schwarz.

Tektronix. 2009. *XYZs of Oscilloscopes*. Application Note.

Tektronix. 2001. *Analyzing Clock Jitter Using Excel*. Application Note.

Tektronix. 2004. *Understanding and Performing Precise Jitter Analysis*. Application Note.

Tektronix. 2000. *Automatic Measurement Algorithms and Methods for the 8000 Series Sampling Oscilloscopes*. Application Note.

van de Plassche, Rudy. 1994. *Integrated Analog-To-Digital and Digital-To-Analog Converters*. The Netherlands: Kluwer Academic Publishers.

Weisstein, Eric. 1999. *Concise Encyclopedia of Mathematics*. Florida: CRC Press.

NOTES

NOTES

NOTES

©2010 Analog Devices, Inc. All rights reserved. Trademarks and registered trademarks are the property of their respective owners.
AN08932-0-4/10(0)